JOURNAL OF RAMAN SPECTROSCOPY, VOL. 26, 407–412 (1995)

Raman Spectroscopy of Bismuth Tungstates

Franklin D. Hardcastle*
Department of Chemistry, Zettlemoyer Center for Surface Studies, Lehigh University, 7 Asa Drive, Bethlehem, Pennsylvania 18015, USA

Israel E. Wachs†
Department of Chemical Engineering, Zettlemoyer Center for Surface Studies, Lehigh University, 7 Asa Drive, Bethlehem, Pennsylvania 18015, USA

The Bi_2O_3–WO_3 system was examined using Raman spectroscopy. The Raman spectra of bismuth tungstate samples having Bi:W ratios of 2:1, 4:1 and 14:1 were used to identify the bismuth tungstate phases present at these compositions. The bismuth tungstate phases which occur were found to depend on the Bi:W ratio. The 2:1 composition consists of only the Bi_2WO_6 phase and the 14:1 composition consists almost entirely of the sillenite phase. The 4:1 composition, however, is multi-phase and consists of Bi_2WO_6, the sillenite phase, and another phase referred to as $7Bi_2O_3$–$2WO_3$. The Raman spectra were used to determine the coordination of the tungstate species as well as their W—O bond lengths in each of these phases.

INTRODUCTION

The ternary oxides, which are derived from bismuth oxide, exhibit a variety of interesting physical properties. For example, the tetragonal phases of thin-film bismuth derived vanadates, niobates and tantalates are efficient photoconductors.[1] Bismuth molybdates possess high activities as catalysts in commercially important reactions such as selective oxidations and ammoxidations of alkenes and other hydrocarbons.[2,3] Thin-film bismuth molybdates are effective gas sensors for alcohols and ketones, and may be potentially useful as breathalyser devices.[4] Similar to the bismuth molybdates, the bismuth tungstates have also been examined as catalysts in the oxidation and ammoxidation of unsaturated hydrocarbons.[5] The bismuth tungstates, however, are not as catalytically active as their molybdate counterparts in spite of the similarities in the structural chemistries of tungsten and molybdenum. In order to understand better the nature of the active site in these catalysts, it is of interest to investigate the structural relationships between the Bi_2O_3–MoO_3 and the Bi_2O_3–WO_3 systems and to correlate their catalytic activities with regard to structure and phase composition. Unfortunately, the phases present in these systems are not completely known, much less the molecular structures within these phases, because of the various difficulties encountered with x-ray diffraction of multiphase systems as well as determining the oxygen locations surrounding a metal cation site.

Raman spectroscopy has been shown, over recent years, to be a useful tool in the characterization of the structures of transition metal oxides as bulk phases[6,7] and two-dimensional surface phases.[7,8] The Raman vibrational spectrum depends on the symmetry and the bonding of a transition metal oxide complex and can be used to discriminate between proposed chemical structures. For example, characteristic vibrational bands have been used to determine the tetrahedral coordination of surface rhenium oxide on alumina[9] and surface chromium oxide on alumina, titania and silica supports.[10]

An empirical relationship has recently been established which relates W—O stretching wavenumbers to their bond lengths in tungsten oxide compounds.[11] The procedure used for establishing this correlation is based on the diatomic approximation where each W—O bond is considered as isolated and independent of the rest of the molecule or crystalline lattice. According to the diatomic approximation, the tungsten oxide polyhedra are reduced to an assembly of W—O diatomic functionalities. An empirical relationship between wavenumbers of W—O stretching modes and bond lengths can then be used to determine bond lengths in metal oxides from measured wavenumbers of Raman stretching modes.

In this study, Raman spectroscopy was used to characterize the tungsten environments in the bismuth tungstates of compositional range $2:1 \leq Bi:W \leq 14:1$. The W—O bond lengths of the tungstate species were determined from wavenumbers of Raman stretching modes using the W—O bond length–stretching wavenumber correlation.[11]

EXPERIMENTAL

The bismuth tungstate samples were kindly provided by Professor J. M. Thomas (Davy Faraday Research

* Present address: Westinghouse Electric Corporation, Bettis Atomic Power Laboratory, West Mifflin, PA 15122, USA.
† Author to whom correspondence should be addressed.

CCC 0377–0486/95/060407–06

Received 12 September 1994
Accepted 14 February 1995

Laboratory, The Royal Institution). These compounds were prepared by mixing stoichiometric amounts of α-Bi_2O_3 with WO_3 (both of 99.9% purity), grinding with mortar and pestle in a slurry of acetone, followed by drying in air, and finally heating in flowing oxygen at 840 °C.[12]

Raman spectra of the bismuth tungstate samples were obtained with a Spectra-Physics Model 171 argon ion laser by utilizing about 10–40 mW of 514.5 nm radiation for excitation. The laser intensity was monitored at the sample. The scattered radiation from the sample was directed into a Spex Triplemate Model 1877 spectrometer which was coupled to an intensified photodiode-array and optical multi-channel analyzer (OMA III: Princeton Applied Research, Model 1463). The photodiode array was thermoelectrically cooled to −35 °C. The Raman spectra were collected and recorded using an OMA III dedicated computer and software. The spectral resolution and reproducibility were experimentally determined to be better than 2 cm^{-1}. About 100–200 mg of each bismuth tungstate sample were pressed into a thin wafer about 1 mm thick with a KBr backing. Each sample was mounted on a spinning sample holder (*ca.* 2000 rpm) where a 90° scattering geometry was used. Further details concerning the optical arrangement used in the Raman experiments can be found elsewhere.[8]

THEORY

The diatomic approximation[11] was used to estimate the tungsten–oxygen bond lengths from Raman band positions for the bismuth tungstates. According to the diatomic approximation, all the metal–oxygen bonds sharing a common metal cation are vibrationally independent of one another. Consequently, to a first approximation, the Raman spectrum is simply a superposition of the wavenumbers of W—O stretching modes from the W—O bonds present in the compound. The wavenumber of the W—O stretching mode of each W—O bond is a function only of its bond length. Therefore, the W—O bond length can be determined directly from a measured wavenumber of a W—O stretching mode. Because the diatomic approximation assumes that each W—O oscillator is independent, it does not lead directly to the symmetry species of the vibrational bands or to the analysis of the bending modes and external modes of the crystal. It does, however, lead to a simple and direct way of determining W—O bond lengths from the wavenumbers of W—O stretching modes for tungsten oxide species. The following empirical relationship has been established[11] and expresses W—O bond length R (Å) as a function of measured Raman stretching wavenumber ν (cm^{-1}):

$$R = 0.52576 \ln (25823/\nu) \quad (1)$$

Equation (1) yields a standard deviation of $\pm$ 0.034 Å for the W—O bond length R as determined from an observed Raman stretching wavenumber ν (cm^{-1}). The overall standard deviation of determining a stretching wavenumber from an absolute (without error) bond length is $\pm$ 55 cm^{-1}.

RESULTS

The Raman spectra for the Bi_2O_3–WO_3 samples, which consist of the 2:1, 4:1 and 14:1 Bi:W compositional ratios, are presented in Figs 1–3. The Raman band positions of the various bismuth tungstate phases present in these compositions are given in Table 1. The only phase-pure sample is the 2:1 composition, which consists entirely of Bi_2WO_6.[13–15] The 4:1 and 14:1 compositions are multi-phase. The bismuth tungstate phases present in the 2:1, 4:1 and 14:1 compositions are briefly summarized in this section.

The Raman spectrum of the 2:1 composition (Bi_2O_3–WO_3) is presented in Fig. 1. This composition is phase-pure in Bi_2WO_6[13–15] and, therefore, all the observed Raman bands are assigned to the Bi_2WO_6 phase. The phase purity of this sample is further confirmed by the absence of Raman bands due to other

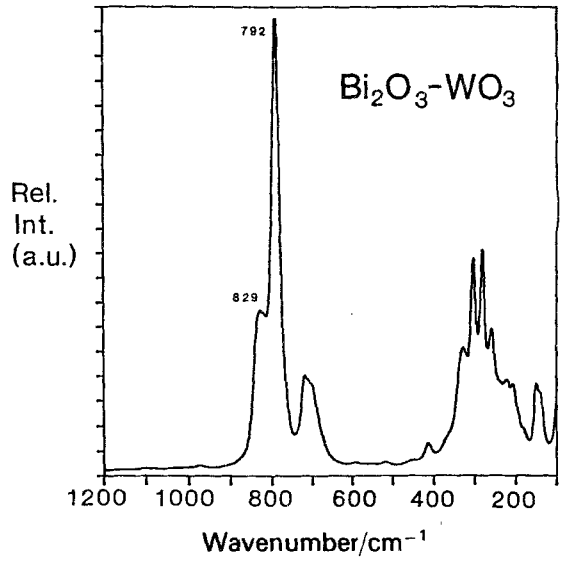

Figure 1. Raman spectrum of Bi_2O_3–WO_3.

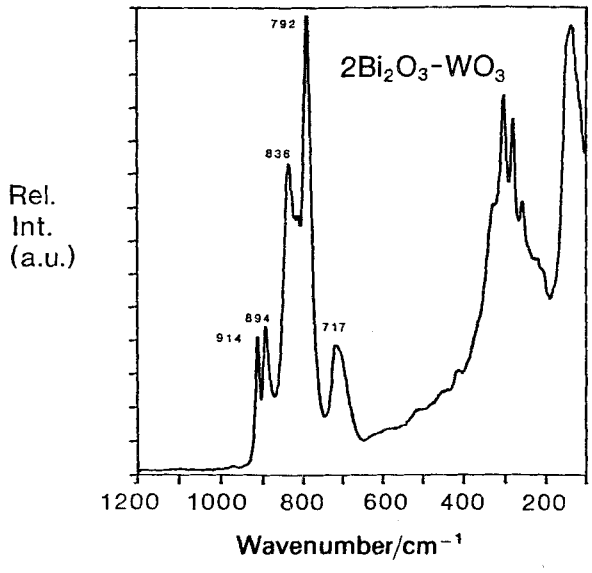

Figure 2. Raman spectrum of $2Bi_2O_3$–WO_3.

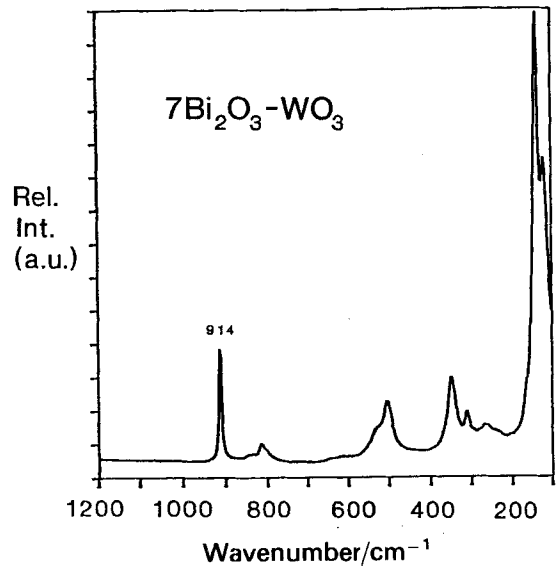

Figure 3. Raman spectrum of $7Bi_2O_3$–WO_3.

bismuth tungstate or bismuth oxide phases. The structure of Bi_2WO_6 is reported to possess alternating layers of $Bi_2O_2^{2+}$ and corner-sharing, distorted WO_6 octahedra (Aurivillius oxide structure).[13] By analogy with the isostructural Bi_2MoO_6 phase,[16,17] there is one type of WO_6 octahedron and two types of BiO_7 polyhedra present in this structure. The W—O bond lengths of the WO_6 octahedra have been determined by neutron diffraction to have two short W—O bonds of 1.69 Å, two intermediate bonds of 1.82 Å and two long bonds of 2.30 Å.[13] These W—O bond lengths have recently been refined using the wavenumbers of the Raman stretching modes and the stretching wavenumber–bond length empirical correlation[11] [Eqn (1)]. The refined W—O bond lengths of Bi_2WO_6 were found to consist of two short bonds of 1.81(3) and 1.83(3) Å, two intermediate bonds of 1.87(3) Å and two long bonds of 2.17(3) and 2.21 Å.[11]

The Raman spectrum of the 4:1 composition is shown in Fig. 2. The 4:1 composition is multi-phase and consists of Bi_2WO_6, $7Bi_2O_3$–$2WO_3$ and a tungsta-stabilized bismuth oxide structure referred to as the sillenite phase, which exhibits well defined and characteristic bands at 620, 531, 440, 372, 262, 205, 154, 146 and 127 cm^{-1}.[18,19] The stabilizing metal oxide tetrahedron in a molybdenum-stabilized sillenite structure occurs at 877 cm^{-1},[20] and the corresponding WO_4 tetrahedron in sillenite is expected to be higher, at 914 cm^{-1};[11] this assignment is confirmed from the Raman spectrum in Fig. 3, which consists almost entirely of the sillenite (see below). The structure and Raman spectrum of the component Bi_2WO_6 have been discussed in the preceding paragraph. The Raman bands not due to either Bi_2WO_6 or the sillenite phase are assigned to the $7Bi_2O_3$–$2WO_3$ phase. Thus, the Raman bands of $7Bi_2O_3$–$2WO_3$ occur at 894, 836, 815 and 717 cm^{-1}. The $7Bi_2O_3$–$2WO_3$ phase has been reported by Hoda and Chang[14] to have a face-centered cubic structure and to possess lattice parameters similar to those of Bi_2WO_6 along two axes. The similarity in lattice parameters suggests a structural relationship between $7Bi_2O_3$–$2WO_3$ and Bi_2WO_6. The structure of the tungstate species in $7Bi_2O_3$–$2WO_3$ is unknown, but is expected to be related to that of Bi_2WO_6. The sillenite phase, also present in the 4:1 composition, is the major component at the 14:1 composition. The sillenite structure is described in the following paragraph.

The Raman spectrum of the 14:1 composition, shown in Fig. 3, shows that this composition consists of almost entirely the sillenite phase (see above), but also contains a trace amount of the $7Bi_2O_3$–$2WO_3$ phase. The sillenite phase is a metal cation, impurity-stabilized bismuth oxide structure which is believed to be isomorphous with pure γ-Bi_2O_3. By comparison, pure γ-Bi_2O_3 is metastable and is observed only at 639 °C by cooling from the high-temperature form of bismuth oxide, δ-Bi_2O_3.[21] At lower temperatures, however, the γ-Bi_2O_3 structure is stabilized by quadrivalent and pentavalent metal cation impurities, giving rise to the sillenite structure. Hexavalent metal cations such as Mo^{6+} and W^{6+}, however, are reported not to cause sillenite phases to form.[22] Nevertheless, the characteristic Raman bands of the sillenite structure have been observed in a Bi:Mo (14:1) composition[20] and are observed for the bismuth tungstates in this study (14:1 composition). The wavenumbers of the Raman bands for the sillenite phase are given in Table 1.

DISCUSSION

In this section, the details of the tungsten coordination that can be inferred from the interpretation of the Raman data for Bi_2WO_6, $7Bi_2O_3$–$2WO_3$ and the sillenite phase are discussed. Of these three phases, the

Table 1. Summary of the Bi_2O_3–WO_3 Raman band positions

Bi:W	Phase	Band positions[a], $\tilde{\nu}$/cm^{-1}
2:1	Bi_2WO_6	829 (s), 792 (vs), 712 (m), 704 (m,sh), 597 (vw), 520 (vw), 452 (vw), 416 (w), 331 (m), 306 (s), 284 (s), 260 (m), 224 (m), 209 (m), 181 (w), 152 (m), 144 (m,sh), 96 (m)
4:1	Bi_2WO_6	792 (vs), 717 (m,br), 595 (vw), 516 (vw), 453 (vw), 414 (w), 328 (m,sh), 306 (s), 282 (s), 259 (m), 219 (w,sh), 205 (w,sh), 181 (w)
	$7Bi_2O_3$–$2WO_3$	894 (m), 836 (s), 815 (w), 717 (m,br)
	Sillenite	914 (m), 140 (vs), 118 (s,sh)
14:1	Sillenite	914 (s), 620 (w), 534 (m,sh), 505 (m), 350 (m), 312 (m), 286 (w,sh), 264 (w,br), 242 (w,sh), 140 (vs), 120 (vs), 95 (s,sh)
	$7Bi_2O_3$–$2WO_3$	895 (vw,sh), 840 (vw), 817 (w), 718 (vw,br)

[a] vw = Very weak; w = weak; m = medium; s = strong; vs = very strong; sh = shoulder; br = broad.

structure of the tungsten oxide species has been determined only for Bi_2WO_6.[13] The bond distances for Bi_2WO_6 have also recently been redetermined using Raman spectroscopy.[11] In this study, the coordination and bond lengths of the tungstate species were determined for $7Bi_2O_3$–$2WO_3$ and the sillenite phase by Raman spectroscopy. The bond lengths were directly determined from the wavenumbers of stretching modes using the W—O correlation [Eqn (1)].

The procedure for determining the W—O bond lengths of a tungstate polyhedron is as follows: (1) determine the coordination of the polyhedron from the Raman spectrum and/or, if possible, by other experimental techniques; (2) identify the W—O stretching bands of the tungstate species; (3) convert all stretching wavenumbers belonging to this species to bond strengths (in valence units) by using the W—O correlation [Eqn (1)] and the empirical relationship of Brown and Wu;[23] (4) calculate the sum of every possible combination of these bond orders (valence sum rule); (5) select those combinations of bond orders having sums which are closest to the formal oxidation state of the metal cation (6.0 ± 0.2 valence units for W^{6+})[11]; and finally, (6) convert the bond orders for those structures having the appropriate valence state ($6.0 + 0.2$ v.u.) into bond lengths by using the stretching frequency–bond length correlation [Eqn (1)]. This procedure leads to the most probable tungstate structures as derived from the Raman data. In the event of more than one equally probable tungstate structure, a hybrid structure is postulated and the error associated with the bond lengths is accordingly increased to accommodate the range of probable structures.

Bi_2WO_6

The structure of Bi_2WO_6 is very similar to that of Bi_2MoO_6. The crystal structure of Bi_2WO_6 is orthorhombic with lattice parameters $a = 5.475$, $b = 5.436$ and $c = 16.427$ Å.[13] There are four formula units per unit cell. On a molecular level, the structure consists of alternating layers of $Bi_2O_2^{2+}$ and corner-sharing and distorted WO_6 octahedra (Aurivillius oxide structure). By analogy, the Bi_2MoO_6 phase (koechlinite) has very similar crystallographic parameters where the orthorhomic cell has lattice parameters of $a = 5.4822(3)$, $b = 5.5091(3)$ and $c = 16.1986(8)$ Å, and there are four formula units per unit cell.[16,17] The molecular structure of Bi_2MoO_6 is also described as having an Aurivillius oxide layered structure with alternating layers of $Bi_2O_2^{2+}$ and corner-sharing, distorted MoO_6 octahedra.

The bond lengths of the WO_6 octahedron in Bi_2WO_6 and the MoO_6 octahedron in Bi_2MoO_6 have been determined by Raman spectroscopy. The Mo—O bond lengths in Bi_2MoO_6 were refined[20] using those values reported from neutron diffraction data to assign the Mo—O stretching modes,[17] the corresponding wavenumbers of Raman stretching modes and an Mo—O empirical correlation relating the wavenumber of Mo—O stretching modes to bond length.[24] These refined Mo—O bond lengths for the MoO_6 octahedron in Bi_2MoO_6 consist of two short bonds of 1.766(16) Å, two intermediate bonds of 1.797(16) and 1.849(16) Å and two longer bonds of 2.222(16) and 2.280(16) Å. The Raman spectra of Bi_2WO_6 (Fig. 1) and Bi_2MoO_6[20] are almost identical, and this similarity was used to assign the stretching W—O Raman bands in the spectrum of Bi_2WO_6.[11] The Mo—O stretching modes used to determine bond distances in Bi_2MoO_6 are at 846, 793, 324 and 292 cm^{-1}.[20] By comparison, the W—O stretching modes used to determine the W—O bond distances in Bi_2WO_6 are at 829, 712, 331 and 306 cm^{-1} (see Fig. 1 and Table 1). From the assigned W—O stretching modes, the W—O bond lengths of Bi_2WO_6 were determined to be 1.810(34), 1.834(34), 1.874(34) × 2, 2.169(34) and 2.210(34) Å.[11] Hence the WO_6 octahedron in Bi_2WO_6 is structurally similar to the MoO_6 octahedron in Bi_2MoO_6, as their Raman spectra show.

$7Bi_2O_3$–$2WO_3$

This phase has been identified by Hoda and Chang[14] as a face-centered cubic structure with lattice parameter $a = 5.51$ Å. The $7Bi_2O_3$–$2WO_3$ was also characterized by Gal'perin *et al.*,[15] and the 4:1 composition showed a cubic lattice parameter of 5.546 Å. Gal'perin *et al.* further compared the structure of this phase with that of δ-Bi_2O_3. The cell dimension of $7Bi_2O_3$–$2WO_3$ is roughly equivalent to that of Bi_2WO_6 along two axes, and this similarity suggests a structural relationship between the two phases. The molecular structure of the tungstate species in $7Bi_2O_3$–$2WO_3$ was not determined by these investigators.

The Raman bands associated with the $7Bi_2O_3$–$2WO_3$ phase are not obvious from the spectrum of the 4:1 composition in Fig. 2. This is because of the coexistence of three bismuth tungstate phases at this composition and the overlap of bands. The three phases present at the 4:1 composition are Bi_2WO_6, $7Bi_2O_3$–$2WO_3$ and the sillenite phase. The Raman band positions for each of these phases are listed in Table 1. The $7Bi_2O_3$–$2WO_3$ phase is also present at the 14:1 composition, although at trace levels, but there is not much overlap with the bands from the sillenite phase. Examination of the Raman spectra of the 4:1 and 14:1 compositions allows the identification of the Raman bands due to the tungstate species in the $7Bi_2O_3$–$2WO_3$ phase. These Raman bands occur at 894, 836, 817 and 718 cm^{-1}.

The wavenumbers of Raman stretching modes at $7Bi_2O_3$–$2WO_3$ lead to the determination of the structure of the tungstate species in this phase. The wavenumbers of W—O stretching modes at 894, 836, 817 and 718 cm^{-1} are due to a WO_6 octahedron and not a WO_4 tetrahedron, because a tetrahedron would exhibit its most intense stretching wavenumber as a single band at *ca* 900 cm^{-1} or higher.[11] The band at 894 cm^{-1} is consistent with the W—O stretch of a perfect WO_4 tetrahedron within the error associated with the W—O correlation [Eqn (1)]. The perfect WO_4 tetrahedron is expected to exhibit an extremely sharp stretching mode at 917 ± 16 cm^{-1} (the lowest observed W—O stretch for a WO_4 tetrahedron occurs at 902 cm^{-1} for $PbWO_4$).[11] While the band at 894 cm^{-1} is consistent with that of a perfect tetrahedron, it is accompanied by additional Raman bands at 836, 817 and 718 cm^{-1}. If all of these bands are due to one tungstate species, then the tungstate species in $7Bi_2O_3$–$2WO_3$ cannot be a

WO_4 tetrahedron. Hence the tungstate species in $7Bi_2O_3$–$2WO_3$ must be a WO_6 octahedron.

The wavenumbers of the stretching modes of the WO_6 octahedron in $7Bi_2O_3$–$2WO_3$ are used to determine its W—O bond lengths. The four stretching wavenumbers at 894, 836, 815 and 717 cm^{-1} are converted into W—O bond orders of 1.453, 1.337, 1.294 and 1.111 valence units, respectively, by the empirical relationship of Brown and Wu.[23] If we assume a WO_6 octahedron with a structure similar to that of Bi_2WO_6, as indicated by their similar lattice parameters, then these bond orders represent the two short and two intermediate W—O bonds of the WO_6 octahedron in $7Bi_2O_3$–$2WO_3$. Subtracting these bond order contributions from the total valence state of the W^{6+} cation leaves a bond order of *ca* 0.4 valence units for each of the two long bonds of the octahedron. The length of these two long Mo—O bonds is approximated because the Raman spectrum of $7Bi_2O_3$–$2WO_3$ does not show bands corresponding to the two long bonds. Thus, the W—O bond lengths of the WO_6 octahedron in $7Bi_2O_3$–$2WO_3$ are accordingly determined to be 1.789(34), 1.814(34), 1.824(34), 1.871(34) and 2.22(4)(× 2) Å by Eqn (1).

The WO_6 octahedron in $7Bi_2O_3$–$2WO_3$ is more distorted than that in Bi_2WO_6 and may, in fact, be thought of in terms of a 4 + 2 coordination with four W—O bonds in the inner coordination sphere and two in the outer coordination sphere. The inner coordination sphere is that of a WO_4 tetrahedron with one short bond, 1.79 Å, two intermediate bonds, 1.81 and 1.82 Å, and one long bond at 1.87 Å. The outer coordination sphere consists of two very long W—O bonds at >2.2 Å which complete the octahedral coordination. This 4 + 2 coordination of the WO_6 octahedron in $7Bi_2O_3$–$2WO_3$ is consistent with the continuous change in structure of the tungstate species as the Bi:W ratio is increased. At the 2:1 composition the tungstate species is a slightly distorted octahedron. In the $7Bi_2O_3$–$2WO_3$ phase, the coordination of the tungstate species is between that of an octahedron and a tetrahedron at 4 + 2 coordination. At the 14:1 composition, where the sillenite phase is formed, the tungstate species is a perfect tetrahedron.

Sillenite

The 14:1 composition has been characterized by Hoda and Chang[14] to consist of a single phase possessing a tetragonal face-centered structure with lattice parameters of $a = 5.52$ and $c = 17.39$ Å. Gal'perin *et al.*[15] classified this phase as a superstructure of the cubic Bi_2O_3 with the c axis tripled. The structure of the tungstate and bismuth oxide polyhedra have not been investigated.

The Raman spectrum of the 14:1 composition, shown in Fig. 3, shows the diagnostic bands of the sillenite phase. This observation is surprising in view of the claims in the literature[22] that hexavalent metal cations such as Mo^{6+} and W^{6+} do not form sillenite phases with bismuth oxide.

The most ideal sillenite structures are those containing quadrivalent metal cations, e.g. in $Bi_{12}GeO_{20}$ and $Bi_{12}SiO_{20}$,[25] because cations such as Ge^{4+} and Si^{4+} lead to structures containing no vacancies in the sillenite structure. The metal cations occupy perfect tetrahedral sites in the sillenite structure. The sillenite structure has also been stabilized by pentavalent cations such as P^{5+}, As^{5+}, V^{5+} and Bi^{5+} and the Raman spectra of these have been reported.[18] Although hexavalent metal cations such as Mo^{6+} and W^{6+} are reported not to cause sillenite phases to form,[22] the characteristic Raman bands of the sillenite structure have been observed in a 14:1 Bi:Mo composition[20] and are observed in the Raman spectrum of the 14:1 Bi:W composition shown in Fig. 3 and listed in Table 1.

Whereas the MoO_4 tetrahedron in the sillenite structure of the Bi:Mo system is slightly distorted,[20] the WO_4 tetrahedron in the tungsten-stabilized sillenite structure is very regular. This conclusion is based on the results from an earlier study where the stretching wavenumber of the perfect WO_4 tetrahedron was predicted to occur at 917 ± 16 cm^{-1}, and the most perfect WO_4 tetrahedron identified by Raman spectroscopy has been found in $PbWO_4$, where the W—O stretch occurs at 902 cm^{-1}.[11] The stretching wavenumber for the WO_4 tetrahedron in the sillenite phase, occurring as a sharp band at 914 cm^{-1}, is higher than that observed for $PbWO_4$, but lies within the range expected for a very regular tetrahedron. Therefore, the WO_4 tetrahedron in the tungsta-stabilized sillenite structure is very regular, but not perfect. The stretching wavenumber of the very regular tetrahedron in the sillenite phase is expressed as a W—O bond length of 1.781(34) Å by Eqn (1).

The tungsten-stabilized sillenite phase can be compared with the molybdenum-stabilized sillenite phase, which exhibits a very similar Raman spectrum.[20] The 14:1 composition of the Bi:Mo system contains a slightly distorted MoO_4 tetrahedron with three Mo—O bonds of 1.748(16) Å and one of 1.787(22) Å. Its stretching wavenumber occurs at 877 cm^{-1}, whereas that of a perfect MoO_4 tetrahedron is predicted to occur at 858 cm^{-1}. The similarity of the Raman spectra of the 14:1 compositions in the Bi:W and the Bi:Mo systems reflects the similar structural behavior of isolated molybdate or tungstate species in a bismuth oxide matrix.

The structural chemistry of tungsten and molybdenum is similar and it is therefore of interest to compare the structural similarities between the bismuth molybdate[20] and bismuth tungstate systems. At the 2:1 compositions, the structures of the molybdate and tungstate species are very similar. At higher bismuth concentrations, however, the bismuth molybdate system contains the $Bi_6Mo_2O_{15}$ and $Bi_{38}Mo_7O_{78}$ phases, both having slightly distorted MoO_4 tetrahedra, while the corresponding bismuth tungstate system contains the $7Bi_2O_3$–$2WO_3$ phase which has a WO_6 octahedron with 4 + 2 coordination. Further, the β- and δ-phases of Bi_2O_3 are identified in the bismuth molybdate system, but not in the bismuth tungstate system. At the 14:1 compositions, however, both systems assume the sillenite structure and the MoO_4 and WO_4 tetrahedra become very regular. Clearly, the bismuth molybdate and tungstate systems are structurally similar at low (2:1) and high (14:1) compositions. At intermediate compositions, however, the phases and structures of the molybdate and tungstate species are very different.

These different bismuth oxide and ternary bismuth oxide phases, which occur at intermediate compositional ratios ($2:1 < Bi:M < 14:1$), are probably responsible for the differences observed in the catalytic activities of the bismuth molybdates and bismuth tungstates.

CONCLUSION

The Bi_2O_3–WO_3 system, in the compositional region $2:1 \leq Bi:W \leq 14:1$, has been examined using Raman spectroscopy. Three distinct bismuth tungstate phases have been identified and the compositional regions of their existence established. In addition to detecting the phases present at each Bi:W composition, the Raman spectra permitted the structural determination of the tungstate species in these phases. The 2:1 composition consists of only the Bi_2WO_6 phase, and the 14:1 composition consists almost entirely of the sillenite phase. The 4:1 composition, however, is multi-phase and consists of Bi_2WO_6, the sillenite phase and another phase referred to as $7Bi_2O_3$–$2WO_3$. The tungstate species in the Bi_2WO_6 phase is that of a slightly distorted WO_6 octahedron, while that in the sillenite phase is a very regular WO_4 tetrahedron. The phase which occurs at intermediate Bi:W compositions, $7Bi_2O_3$–$2WO_3$, consists of a WO_6 octahedron with 4 + 2 oxygen coordination, that is, an inner coordination sphere with four W—O bonds and an outer coordination sphere with two W—O bonds. The W—O bond lengths of the tungstate species present in each of these phases are given in Table 2.

The diatomic approximation, which provides the basis of the W—O empirical correlation between wavenumbers of Raman stretching modes and W—O bond length, was used to determine the W—O bond lengths of the tungstate species in the three bismuth tungstate phases. The diatomic approximation is a powerful tool in the interpretation of Raman spectra of metal oxide species. In cases where diffraction techniques are incapable of providing oxygen positions, Raman spectroscopy may be used to generate vital structural information. It is firmly believed that such an approach will popularize Raman spectroscopy as a complementary technique to be used routinely with diffraction methods in structural investigations of transition metal oxide systems.

Table 2. W—O bond lengths of tungstate species in bismuth tungstate phases

Phase	Bond to W	W—O/Å (±0.3 Å)
Bi_2WO_6	O(1)	1.81
	O(2)	1.83
	O(3)	1.87
	O(4)	1.87
	O(5)	2.17
	O(6)	2.21
$7Bi_2O_3$–$2WO_3$	O(1)	1.79
	O(2)	1.81
	O(3)	1.82
	O(4)	1.87
	O(5)	2.22
	O(6)	2.22
Sillenite	O(1–4)	1.78

Acknowledgements

Financial support from the Texaco Philanthropic Foundation and from the Sherman Fairchild Foundation is gratefully acknowledged by F.D.H. We thank Professor J. M. Thomas (Davy Faraday Research Laboratory, The Royal Institution) for providing the bismuth tungstate samples.

REFERENCES

1. T. Sekiya, A. Tsuzuki and Y. Torii, *Mater. Res. Bull.* **20**, 1383 (1985).
2. J. M. Thomas, D. A. Jefferson and G. R. Millward, *JEOL News* **23E**, 7 (1985).
3. D. A. Jefferson, J. M. Thomas, M. K. Uppal and R. K. Grasselli, *J. Chem. Soc., Chem. Commun.* 594 (1983).
4. N. Hykaway, W. M. Sears, R. F. Frindt and S. R. Morrison, *Sensors Actuators* **15**, 105 (1988).
5. I. K. Kolchin, E. L. Gallperin, S. S. Bobokov and L. Y. Margolis, *Neftekhimiya* **5**, 111 (1965).
6. N. Nakamoto, *Infrared and Raman Spectra of Inorganic and Coordination Compounds*, 3rd ed. Wiley, New York (1978).
7. L. Dixit, D. L. Gerrard and H. J. Bowley, *Appl. Spectrosc. Rev.* **22**, 189 (1986).
8. I. E. Wachs, F. D. Hardcastle and S. S. Chan, *Spectroscopy* **1**, 30 (1986).
9. F. D. Hardcastle, I. E. Wachs, J. A. Horsley and G. H. Via, *J. Mol. Catal.* **46**, 15 (1988).
10. F. D. Hardcastle and I. E. Wachs, *J. Mol. Catal.* **46**, 173 (1988).
11. F. D. Hardcastle and I. E. Wachs, *J. Raman Spectrosc.*, **26**, 397 (1995).
12. D. J. Buttrey, D. A. Jefferson and J. M. Thomas, *Mater. Res. Bull.* **21**, 739 (1986).
13. R. W. Wolfe, R. E. Newnahm and M. I. Kay, *Solid State Commun.* **7**, 1797 (1969).
14. S. N. Hoda and L. L. Y. Chang, *J. Am. Ceram. Soc.* **57**, 323 (1974).
15. E. L. Gal'perin, L. Y. Erman, I. K. Kolchin, M. A. Belova and K. S. Chernyshev, *Russ. J. Inorg. Chem.* **11**, 1137 (1966).
16. A. F. Van den Elzen and G. D. Rieck, *Acta Crystallogr., Sect. B* **29**, 2436 (1973).
17. R. G. Teller, J. F. Brazdil, R. K. Grasselli and J. D. Jorgensen, *Acta Crystallogr., Sect. C* **40**, 2001 (1984).
18. M. Devalette, J. Darriet, M. Couzi, C. Mazeau and P. Hagenmuller, *J. Solid State Chem.* **43**, 45 (1982).
19. S. Venugopalan and A. K. Ramdas, *Phys. Rev. B* **5**, 4065 (1972).
20. F. D. Hardcastle and I. E. Wachs, *J. Phys. Chem.* **95**, 10763 (1991).
21. H. A. Harwig, *Z. Anorg. Allg. Chem.* **444**, 151 (1978).
22. Y. F. Kargin, A. A. Mar'in and V. M. Skorikov, *Izv. Akad. Nauk SSSR, Neorg. Mater.* **18**, 1605 (1982).
23. I. D. Brown and K. K. Wu, *Acta Crystallogr., Sect. B* **32**, 1957 (1976).
24. F. D. Hardcastle and I. E. Wachs, *J. Raman Spectrosc.* **21**, 683 (1990).
25. S. C. Abrahams, P. B. Jamieson and J. L. Bernstein, *J. Chem. Phys.* **47**, 4034 (1967).